

ACTIVE CONTOUR SEGMENTATION FOR THE IDENTIFICATION OF METALLOGRAPHIC AND MORPHOLOGICAL ELEMENTS OF INTEREST IN DUCTILE CAST IRON

F. Iacoviello, A. De Santis, D. Iacoviello, O. Di Bartolomeo

Ductile cast irons are characterized by a wide range of mechanical properties that depend on graphite elements morphology and microstructure properties. Both chemical composition and manufacturing conditions control matrix microstructure, and ferritic, pearlitic, ferritic-pearlitic, martensitic, bainitic, austenitic and austempered ductile irons can be obtained. Considering crack propagation resistance of ductile cast irons, their peculiar behaviour is due to the graphite elements shape, that is approximately spheroidal. Due to their morphology, graphite elements can act as crack arresters: as a consequence ductile cast irons are characterized by high ductility and toughness values and can be used for loading conditions that could be considered as critical for other cast irons types (e.g. fatigue loading conditions).

Up to some years ago, microstructure analysis was mainly performed by means of semi-quantitative procedures applied to metallographically prepared specimens, with the characteristics evaluation that was mainly based on the operator expertise. Only recently there has been an increasing interest in numerical procedures of image analysis for quantitative evaluation of materials. In this work the problem of the estimation of the morphological parameters of elements such as graphite nodules, domains of chemical etching and metallic matrix has been taken up by a variational approach of image segmentation by active contours.

Considering ductile irons, images obtained by means of a light optical microscope (LOM) on metallographically prepared specimens show both graphite elements (spheroids, nodules, lamaellas etc.) and microstructure elements (ferrite grains, pearlite lamaellas, etc.) and some artefacts due the preparing procedure that should be distinguished by more interesting elements. An automatic identification procedure is here proposed to distinguish the nodules from the metallic matrix and to evaluate the nodules shape parameters of interest and the composition of the metallic matrix (ferrite/pearlite volume fraction).

KEYWORDS: cast iron, fatigue, metallography

INTRODUCTION

Ductile cast irons could be considered as ternary Fe-C-Si alloys, characterized by C and Si content that range between 3.5-3.9% and 1.8-2.8% respectively. Chemical composition selection is usually

determined by casting size, considering the required mechanical properties. Graphite elements are characterized by a nodule-like shape and their nucleation and growth are characterized by the alloy purity level and by the spheroidizing elements addition [1]. Graphite elements usually nucleate corresponding to some inclusions (e.g. MgS, CaS, SrS, MgO), and they grow by means of a carbon solid state diffusion mechanism, through the austenite shields around graphite spherulites [2, 3]. Graphite elements morphology and matrix microstructure determine the ductile cast irons mechanical properties. Graphite elements can act as crack arresters: as a consequence ductile cast irons are characterized by

F. Iacoviello, O. Di Bartolomeo

Università di Cassino, Di.M.S.A.T., Cassino (FR)

A. De Santis, D. Iacoviello

Università di Roma "La Sapienza", DIS "Antonio Ruberti", Roma

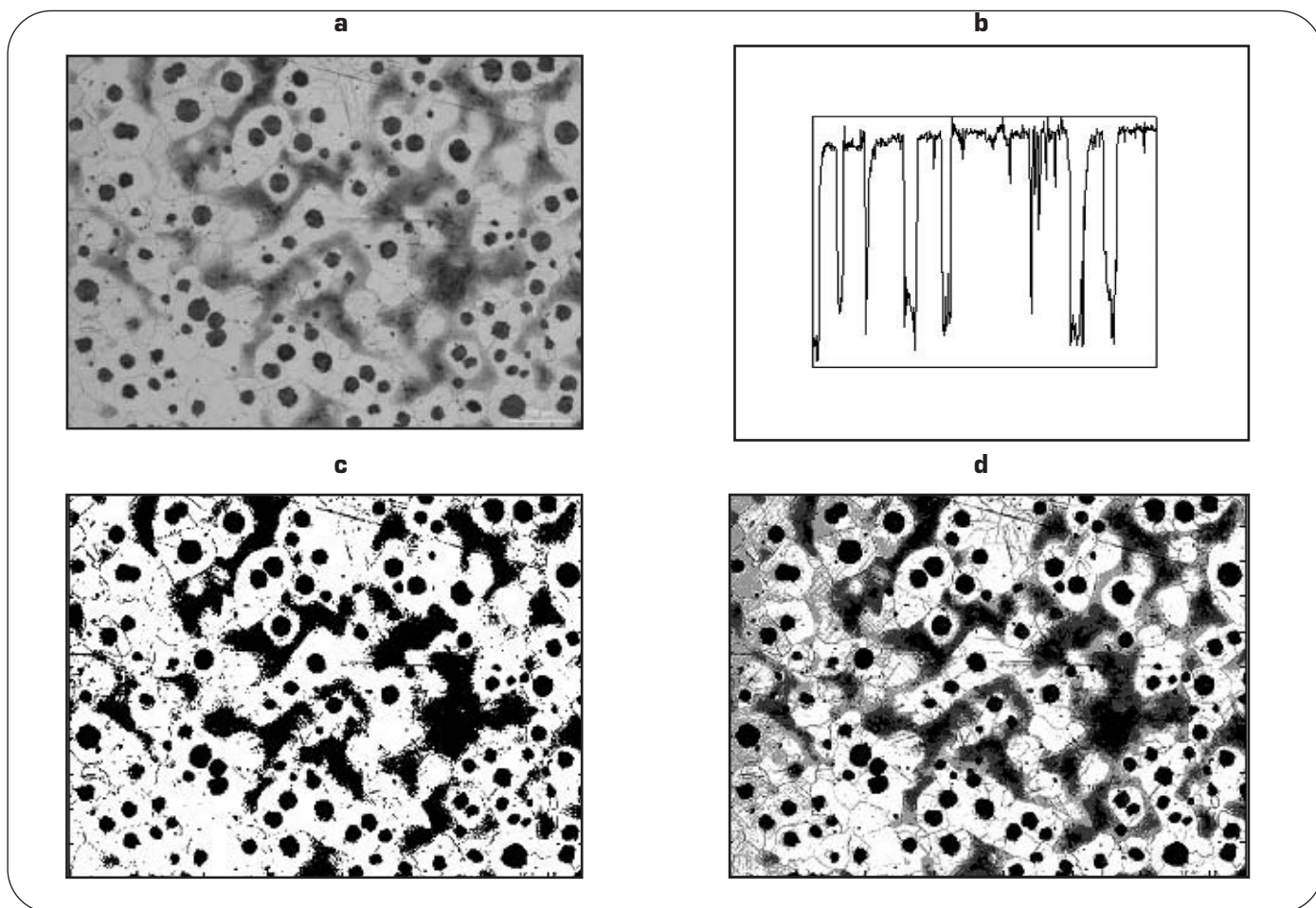


Fig. 1

a) metallographic specimen original image; b) gray level variation along a row of the image a); c) two-levels segmentation ; d) four-levels segmentation.

a) Immagine originale di un provino metallografico; b) andamento del livello di grigio di una riga dell'immagine a); c) segmentazione con 2 livelli; d) segmentazione con 4 livelli.

high ductility and toughness values and they can be used for loading conditions that could be considered as critical for other cast irons types (e.g. fatigue loading conditions). This interesting result is obtained only for a very high nodularization of graphite elements. A degeneration of the graphite elements implies a deterioration of the ductile cast iron mechanical properties: for instance the graphite elements not working as crack arrester could generate secondary cracks [4].

Graphite nodules geometrical characteristics are usually controlled according to ASTM standard [5] or analogous: proposed procedures are essentially based on a semi-quantitative analysis of graphite elements size, nodularity degree and distribution; the results are strongly affected by the operator expertise.

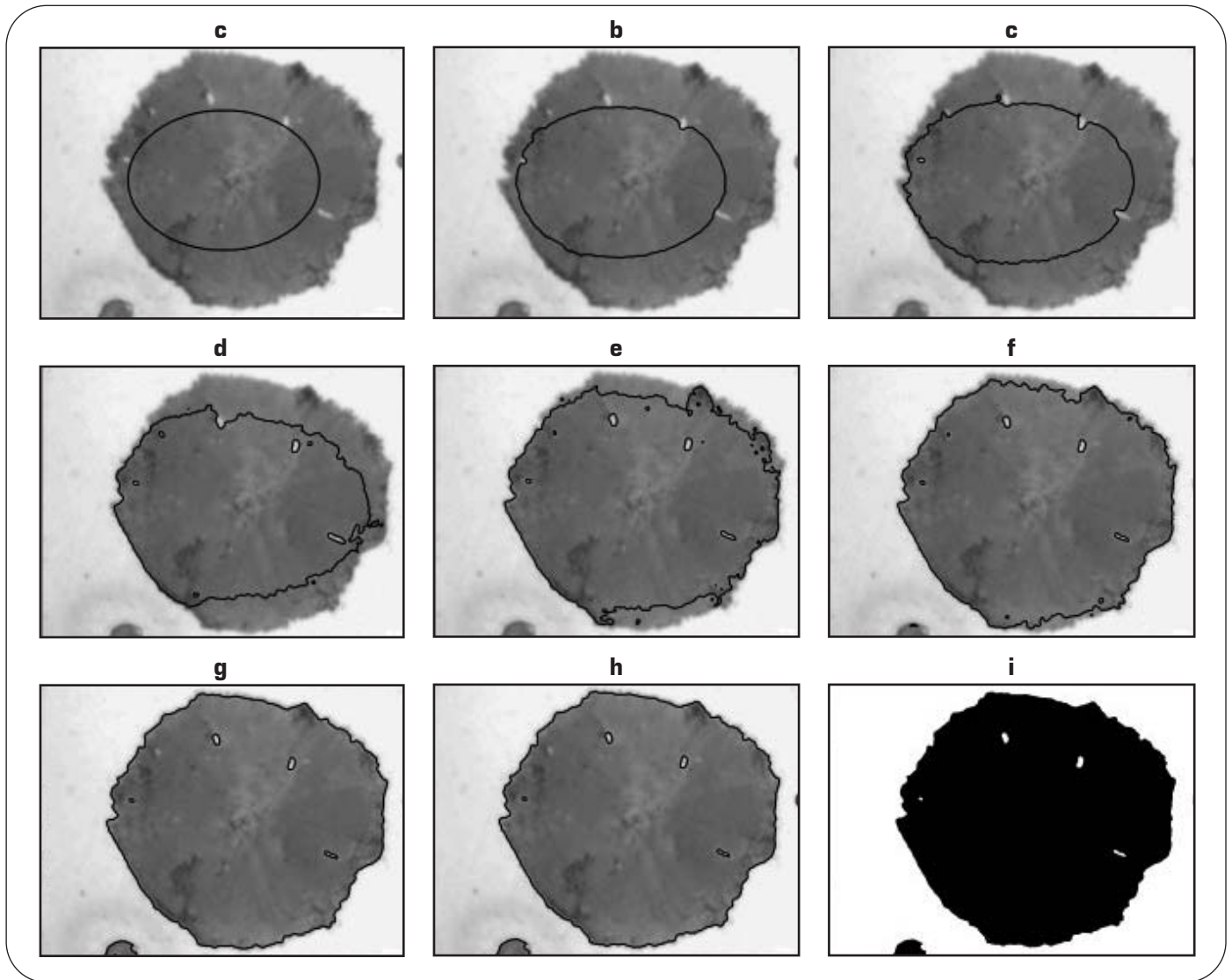
With the support of image processing software, various procedures have been designed for *quantitative metallography*. By analysing metallographic specimens, statistical evaluations of quantities such as the number of particles per unit volume, grains size, phases volume fractions, are performed. Numerous shape factors have been proposed in the quantitative analysis of spheroids [6], such as the S_{AA} factor defined as the ratio between the area S of the nodule's section and the area S_0 of the circumscribing circle. This is currently one of the most used shape factors [7], even though it describes only the degree of nodularization of the spheroid section but not its roundness. In this paper the problem of

identification and characterization of the graphite nodules and the distribution (phases volume fractions) of the metallic matrix have been considered and a novel quantitative analysis procedure has been developed based on a segmentation with active contours technique [8, 9]. This is a methodology for image analysis of the material metallographic specimens pictures, that provides a reliable and efficient separation of the elements of interest from the background and the evaluation of their morphological characteristics.

ACTIVE CONTOUR SEGMENTATION

LOM images of ductile cast irons metallographic planes show, along with the spheroids and the metallic matrix, irregular objects and artefacts (waxing scratches, oxidation albedoes) due to the specimen preparation procedure and data acquisition; these have to be distinguished from the elements of interest. The experimental data for a generic metallographic specimen is given by a 8-bit digital image represented by an array of integer numbers encoding 256 gray levels, conventionally belonging to the interval [0, 1]. Any of the array entry provides the gray level value of the corresponding image pixel. The array therefore provides a digital and quantized representation of the LOM data.

The automatic (unsupervised) analysis of the metallographic spec-



▲
Fig. 2

a)-h) active contour evolution from the initial configuration to the final one;

i) two-levels segmentation.

a)-h) evoluzione del contorno attivo dalla configurazione iniziale a quella finale;

i) segmentazione con 2 livelli.

iments pictures is far from trivial: the elements of interest (nodules, zones of chemical etching, metallic matrix features) are generally not well separated one to each other and from the background artefacts to be well identified by simple thresholding procedures, exploiting the gray scale differences. For instance, the nodules are surely the darkest elements in the specimen picture, Fig. 1a); these could be at first easily detected by setting a threshold of 0.3 and classifying the image pixels whose gray level value is not higher than the threshold as belonging to the spheroids. In this way a two-levels segmentation (binarization) of the original image would be obtained: black for the nodules and white for the background. Nevertheless, the chosen threshold for the given specimen may not be suitable for a different specimen. For this reason the segmentation, despite being simple and efficient, would result in a heuristic procedure in the choice of the threshold values requiring the supervision of an expert. Moreover, despite the specimen picture may appear of good quality on visual inspection Fig. 1a), the image signal is highly irregular Fig. 1b) due to the preparation artefacts

and acquisition process. Consequently the threshold may even change within the same picture, this being a serious drawback. Therefore, the identification of the graphic elements useful to the evaluation of the material mechanical properties must be performed with a more sophisticated segmentation technique [10]. This consists in the reduction of the image gray levels number without changing its informative content, in particular without modifying the shape of the elements of interest for our analysis. In this way a simplified image is obtained with all the elements well separated one to another. The number of gray levels in the segmented image depends on the degree of detail needed; usually two levels Fig. 1c), or four levels Fig. 1d), are adequate for the analysis required in metallurgy.

The technique used is based on a variational method that is called *segmentation with active contours* [8, 9]: an initial curve of general shape is evolved on the image plane so to place it exactly on the boundaries of the objects of interest, that therefore can be separated from each other. Referring to Fig. 2, the initial curve divides the

C	Si	Mn	S	P	Cu	Cr	Mg	Sn
3.66	2.72	0.18	0.013	0.021	-	0.028	0.043	0.010

▲
Tab. 1

EN GJS350-22 ductile iron (100% ferrite).

Ghisa sferoidale EN GJS350-22 (100% ferrite).

C	Si	Mn	S	P	Cu	Cr	Mg	Sn
3.65	2.72	0.18	0.010	0.03	-	0.05	0.055	0.026

▲
Tab. 2

EN GJS450-10 ductile iron (70% ferrite - 30% pearlite).

Ghisa sferoidale EN GJS450-10 (70% ferrite - 30% perlite).

C	Si	Mn	Mo	Ni	Sn	S
3.61	2.23	0.32	0,42	0,52	0,045	0,015

▲
Tab. 3

Austempered GGG 70BA ductile iron (fully bainitic).

Ghisa sferoidale austemperata GGG 70BA (completamente bainitica).

image in two domains, the interior and the exterior. The curve is then progressively deformed in such a way that within the two domains the gray level is more homogeneous, whereas it changes drastically on passing from one domain to the other. In Fig. 2h) the final curve configuration defines the segmentation that best separates the spheroid from the background; such a final configuration, and the corresponding segmentation of Fig. 2i), does not depend on the choice of the initial curve, being dependent only on the gray level distribution of the image. The procedure requires neither any update for different images of the same class nor the supervision of an expert; therefore the same algorithm can be used to find the best segmentation for any sample image, also in presence of a different degree of degradation. The algorithm convergence is very fast, and can be implemented on a general purpose PC. The technical details can be found in [9] where an innovative active contour segmentation procedure is presented, whereas a schematic procedure outline is reported in the Appendix.

The proposed procedure has been applied both to the problem of the characterization of the metallic matrix, considering ductile cast irons with ferritic-pearlitic matrix, and to the problem of the characterization of the graphite nodules possible degeneration consequent to a thermal treatment in two different austempered ductile cast irons. In this latter case the results obtained by the active contour segmentation procedure have been compared with those obtained in the tests of fatigue crack propagation, in order to evaluate the sensibility of the proposed procedure and to quantify the influence of the microstructure parameters on the material mechanical behaviour.

MATERIAL AND EXPERIMENTAL PROCEDURE

Performing the matrix microstructure analysis, two ferritic-pearlitic ductile cast irons were considered (Tab. 1

and 2). Ferrite and pearlite volume fractions in table 1 and 2 were empirically evaluated according to ASTM standard.

In order to evaluate the graphite elements degeneration level, two different austempered ductile irons were obtained from the same ferritic-pearlitic ductile iron (Tab. 3), considering two different austempering heat treatments: both heat treatments allowed to obtain the same microstructure (fully bainitic), with different levels of graphite elements degeneration.

Higher graphite elements degeneration level corresponds to ADIA ductile cast iron, obtained with the following heat treatment:

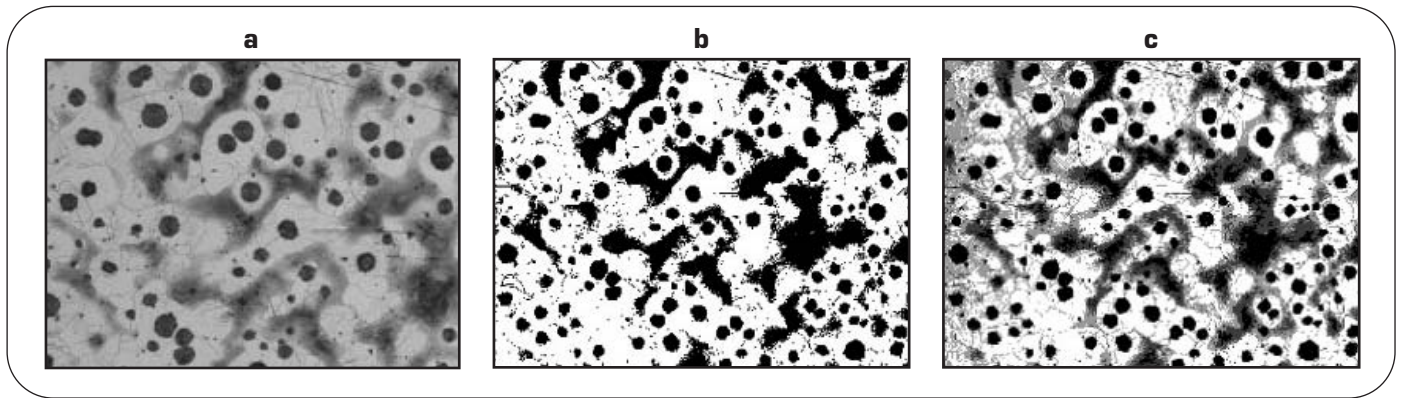
- Annealing at 910°C for 70 minutes;
- Salt bath quench (2 hours at 370°C followed by 60 seconds at 320°C);
- Air cooling up to environment temperature;

Lower graphite elements degeneration level corresponds to AIDB ductile cast iron, obtained with the following heat treatment:

- Annealing at 910°C for 70 minutes;
- Salt bath quench (1 hours at 370°C followed by 60 seconds at 300°C);
- Air cooling up to environment temperature.

Light optical microscope (LOM) observations were performed on metallographically prepared specimens, etched with a Nital 3% for 5 s.

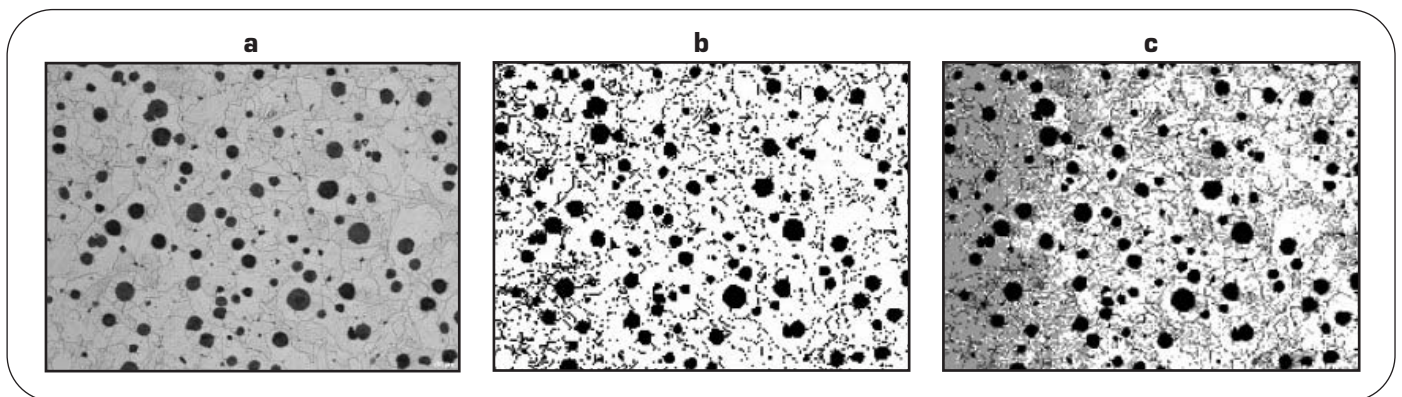
Considering austempered ductile irons, fatigue crack propagation tests were run according to ASTM E647 standard [11], using 10 mm thick CT (Compact Type) specimens and considering three different stress ratio values (e.g. $R = P_{min}/P_{max} = 0.1; 0.5; 0.75$). Tests were performed using a computer controlled INSTRON 8501 servohydraulic machine in constant load amplitude conditions, considering a 20 Hz loading frequency, a sinusoidal loading waveform and laboratory conditions. Crack length measurements were performed by means of a compliance method using a double cantilever mouth gage, and con-



▲
Fig. 3

3 a) original image with 70% of ferrite (visual inspection expert evaluation) ; b) two-levels segmentation; c) four-levels segmentation.

a) immagine originale con 70% di ferrite (valutazione soggettiva fatta da un esperto); b) segmentazione con 2 livelli; c) segmentazione con 4 livelli.



▲
Fig. 4

a) original image with 100% of ferrite (visual inspection expert evaluation) ; b) two-levels segmentation; c) four-levels segmentation.

a) immagine originale con 100% di ferrite (valutazione soggettiva fatta da un esperto); b) segmentazione con 2 livelli; c) segmentazione con 4 livelli.

trolled using an optical microscope (x40). Fracture surfaces were analyzed by means of a scanning electron microscope (SEM).

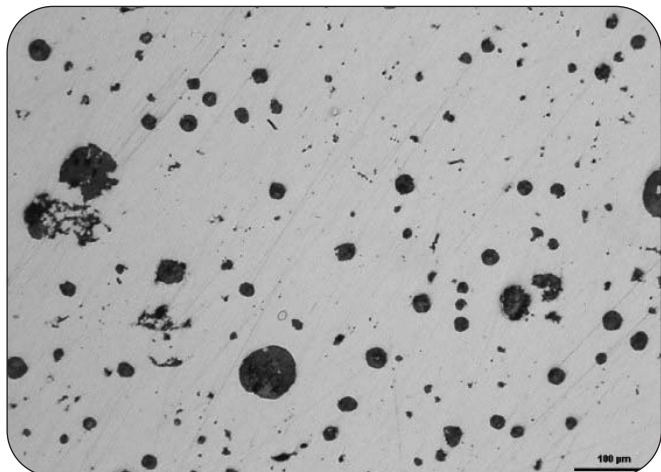
RESULTS AND COMMENTS

By using the segmentation procedure described in [9], for every specimen the two-levels and four-levels segmentations have been obtained. The segmented versions approximate the original image with a piece-wise constant representation; this is obtained by a global optimization procedure that minimizes a cost functional that weighs the approximation error, the area of the segmentation domains and the length of their boundaries (formula (3) in the Appendix).

For the specimen picture reported in Fig. 3a), relative to the cast iron EN GJS450-10, the percentage of ferrite can be evaluated by measuring from Fig. 3b) the ratio between the area of the white zone (corresponding to the ferritic phase of the matrix) and the total area of the metallic matrix (total specimen area minus the nodules areas, that are accurately computed from the four-levels

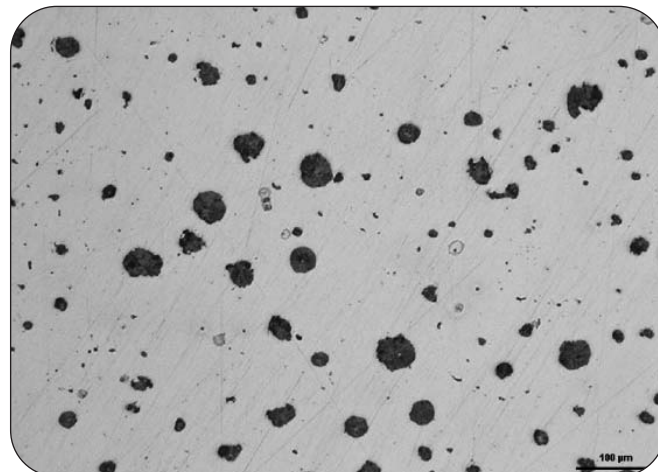
segmentation of Fig. 3c)); indeed, from Fig. 3b) the ferritic phase area can be evaluated by counting the pixels of the binarization white zone, obtaining a value of 75%. We like to stress the accuracy of the separation of the white zone from the rest of the picture; this is mainly due to the *global* character of the procedure that links the value estimated in any pixel to the values in all the others. A simple thresholding procedure, where the value in any pixel depends at most on the values in few neighbouring pixels, would invariably commit many errors in trying to separate the nodules from the background, given the signal of Fig. 3a) with many gray levels. Moreover the proposed segmentation procedure allows us to label and address any single graphic elements of the specimen picture and to analyse it separately from the others. For this reason these kind of global procedures are called *region based*. Local procedures on the contrary determine tick and fragmented object contours, and therefore can not directly define any relation among the pixels of the same object. These procedures are typically *pixel oriented*.

The same global procedure was applied to the specimen picture of Fig. 4), relative to the cast iron EN GJS350-22,



▲
Fig. 5

Graphite elements in austempered ductile iron ADIA.
Elementi di grafite nella ghisa austemperata ADIA.



▲
Fig. 6

Graphite elements in austempered ductile iron ADIB.
Elementi di grafite nella ghisa austemperata ADIB.

estimating a ferrite percentage of 96%. Corresponding to lower applied ΔK and/or R values, matrix microstructure influence on fatigue crack propagation resistance results to be negligible, whereas it becomes quite evident corresponding to higher R values, in the stage II (Paris stage) and in the stage III of fatigue crack propagation [12]. As a consequence, a quantitatively correct identification of ferrite/pearlite volume fraction does not seem to be critical for the stage I of fatigue crack propagation (threshold stage), where graphite elements morphology plays a key role. In this work, this critical parameter was

quantitatively evaluated by applying the proposed global procedure to ADIA and ADIB ductile irons (Fig. 5 and Fig. 6, respectively).

The graphite elements morphology was characterized by the *solidity* and *eccentricity* parameters. The solidity is defined as the ratio between the nodule's area and the area of its convex hull (the smallest polygon that circumscribes it); it has values within [0, 1] and evaluates the spheroid boundary raggedness. A solidity equal to 1 denotes a convex regular shape without inlets. The eccentricity is defined through the ellipses that circum-

		25<Area<250 (pixel)	250<Area<750 (pixel)	Area>750 (pixel)
Number of nodules for area bins		71	6	7
Solidity	mean value	0.8779	0.7478	0.6401
	standard deviatio	0.0625	0.0909	0.1427
Eccentricity	mean value	0.6845	0.7940	0.6680
	standard deviatio	0.1974	0.1394	0.2201

▲
Tab. 4

Graphite elements characterization (ADIB ductile iron).
Quadro riassuntivo relativo agli elementi di grafite (ghisa ADIB).

		25<Area<250 (pixel)	250<Area<750 (pixel)	Area>750 (pixel)
Number of nodules for area bins		40	12	6
Solidity	mean value	0.9039	0.9250	0.9391
	standard deviatio	0.0374	0.0228	0.0359
Eccentricity	mean value	0.6416	0.5644	0.5797
	standard deviatio	0.1460	0.1431	0.1279

▲
Tab. 5

Graphite elements characterization (ADIB ductile iron).
Quadro riassuntivo relativo agli elementi di grafite (ghisa ADIB).

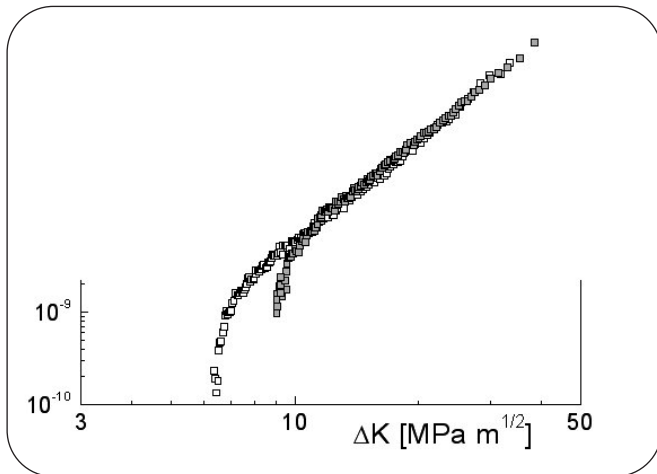


Fig. 7

ADIA and ADIB ductile irons fatigue crack propagation resistance ($R = 0.1$).

Resistenza alla propagazione della cricca di fatica per le due ghise ADIA ed ADIB ($R = 0,1$).

scribes the nodule, and its value is obtained as the ratio between the foci distance and the major axis length. The eccentricity has values within $[0, 1]$ and evaluates how far is the spheroid shape from being circular, the circle having eccentricity equal to zero. The two austempered ductile cast irons have been investigated by analysing 20 pictures for each of them, obtaining the average values reported in Tab. 4 and Tab. 5.

The performed image analysis allows us to highlight and quantify the graphite elements degeneration. Ductile iron ADIA is characterized by lower solidity and higher eccentricity values. The consequence on fatigue crack propagation resistance is shown in Figures 7-9. For all the investigated R values, ADIA ductile iron shows lower ΔK_{th} (ΔK threshold values) if compared with ADIB ductile iron.

Ductile iron microstructure seems to be influenced by different factors, depending on the applied ΔK value:

- Lower applied ΔK values (stage I, threshold stage) imply values of the radius of the cyclic plasticization zone ($r_{pz} = (\Delta K / \sigma_y)^2 / 12\pi$) that are comparable with graphite elements size. Their degeneration could imply a decrease of the fatigue crack propagation resistance, and a consequent decrease of the ΔK_{th} .

- Higher applied ΔK values (stage II, Paris stage and stage III) implies a decrease of the importance of graphite elements, with a consequent increase of matrix microstructure importance because of the increase of the radius of the cyclic plasticization zone ($r_{pz} \propto \Delta K^2$): investigated austempered ductile irons are characterized by the same matrix microstructure and show the same fatigue crack propagation resistance in stage II and III.

Scanning electron microscope (SEM) fracture surface analysis allows the study of the graphite elements degeneration influence on crack propagation micromechanisms. Higher degenerated austempered ductile iron (ADIA, Fig. 10), is characterized by the presence of secondary cracks corresponding to low ΔK values, that propagate from the degenerated graphite elements. Graphite elements - matrix debonding is commonly

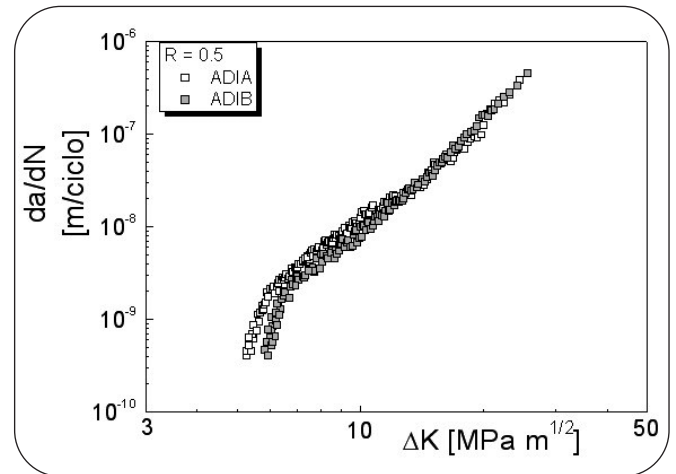


Fig. 8

ADIA and ADIB ductile irons fatigue crack propagation resistance ($R = 0.5$).

Resistenza alla propagazione della cricca di fatica per le due ghise ADIA ed ADIB ($R = 0,5$).

observed. Austempered ductile iron ADIB does not present secondary cracks and graphite elements - matrix debonding seems to be the main damaging micromechanism due to graphite elements presence (Fig. 11).

CONCLUSIONS

The aim of this work was the identification and the characterization of graphite elements in ductile cast irons by means of a novel active contours segmentation procedure. The proposed procedure was able to recognize the graphite nodules contours, and to identify different matrix phases. It was also applied on ferritic-pearlitic ductile irons (in order to identify and quantify matrix phases) and on austempered ductile irons (in order to evaluate graphite elements degeneration degree). The influence of graphite elements degeneration on fatigue crack propagation resistance and on fatigue crack propagation micromechanisms was also investigated. On the basis of the obtained results, the following conclusions can be summarized:

- the proposed image analysis procedure provides a quantitative and objective characterization of both phases volume fractions and graphite elements degeneration degree, avoiding the need for an operator with particular expertise;
- the fatigue crack propagation resistance of ductile cast irons is mainly influenced by matrix microstructure for higher R and or ΔK values, whereas graphite elements degeneration influence is more evident corresponding to lower ΔK values, for all the investigated R values;
- the presence of degenerated graphite elements in ductile cast iron implies the presence of secondary crack as an additional damaging micromechanisms.

REFERENCES

- [1] C. LABRECQUE, M. GAGNE, Canadian Metallurgical Quarterly, 37 (1998) p.343.
- [2] H. MORROGH, The solidification of Metals, The Iron

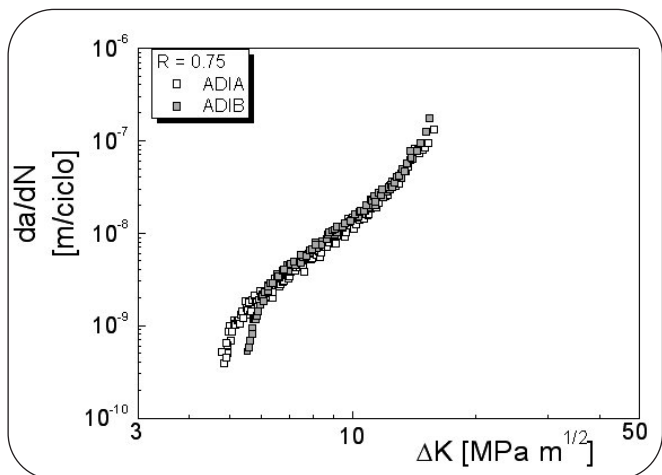


Fig. 9

ADIA and ADIB ductile irons fatigue crack propagation resistance ($R = 0.75$).

Resistenza alla propagazione della cricca di fatica per le due ghise ADIA ed ADIB ($R = 0,75$).

and Steel Institute (1967), p.238.

- [3] T. SKALAND, O. GRONG, T. GRONG, Metall. Trans. A, 24A (1993) p. 2321.
- [4] G.L. GRENO, J.L. OTEGUI, R.E. BOERI, International Journal of Fatigue, 21 (1999) p.35.
- [5] ASTM Designation A445-63T; ASTM Designation A247-67, 1985 Annual Book.
- [6] JIANMING LI, LI LU, MAN ON LAI, Materials Characterization 45 (2000) p.83.
- [7] T.L. CAPELLETTI J.R. HORNADA, AFS Trans. 82 (1974) p.59.
- [8] T.F. CHAN, L. VESE, IEEE Trans. on Image Proc. 10 (2001) 266-277.
- [9] A. DE SANTIS, D. IACOVIELLO, DIS-Rep. n. 1305, submitted to International Journal of Computer Vision.

- [10] J.L. MOREL, S. SOLIMINI, Variational Methods in Image Segmentation, Birkhauser, Boston 1995.
- [11] ASTM Standard test Method for Measurements of fatigue crack growth rates (E647-93), Annual Book of ASTM Standards, 1993, American Society for Testing and Materials.
- [12] F. IACOVIELLO, V. DI COCCO, "Fatigue crack paths in ferritic-perlitic ductile cast irons", Atti del Convegno Internazionale International Conference on Fatigue Crack Paths, Parma 18-20 settembre 2003, n. 116.
- [13] G. AUBERT, L. VESE, "A variational method in image recovery", SIAM J. Numer. Analysis, vol. 34, no. 5, 1997.

APPENDIX

An innovative segmentation procedure formulated in the data discrete domain is outlined. As a particular case of segmentation let us consider a piece-wise constant image representation. Any image I is defined as an array of integers $\{I_{i,j}\}$ on a grid of points $D = \{(i,j), i=1, \dots, N; j = 1, \dots, M\}$. Without loss of generality assume that $I: D \rightarrow [0, 255]$. Let $\{D_k\}$, $k = 1, \dots, K$, be a finite partition of domain D with boundary ∂D ; a piece-wise constant segmentation is defined as follows

$$I_s = \sum_{k=1}^K c_k \chi_{D_k}, \quad \chi_{D_k}(i,j) = \begin{cases} 1 & \text{for } (i,j) \in D_k \\ 0 & \text{otherwise} \end{cases} \quad (1)$$

where $\partial = \{ \cup_{k=1}^K \partial D_k \}$ is the segmentation boundary (note that by definition $\partial D \subset B$), the c_k 's are the constant values assigned to each segmentation sub-domain D_k , chosen in a set of $n_c \leq K$ values. A simple formulation of the segmentation problem is the following: given an image $I: D \rightarrow [0, 255]$, choose an integer $n_c \geq 2$ and find a partition $\{D_k\}$, $k = 1, \dots, K$ of D along with constants c_1, \dots, c_K such that I_s in (1) is a good representation of I according to a suitable optimality criterion.

A reasonable criterion consists in the optimization of the

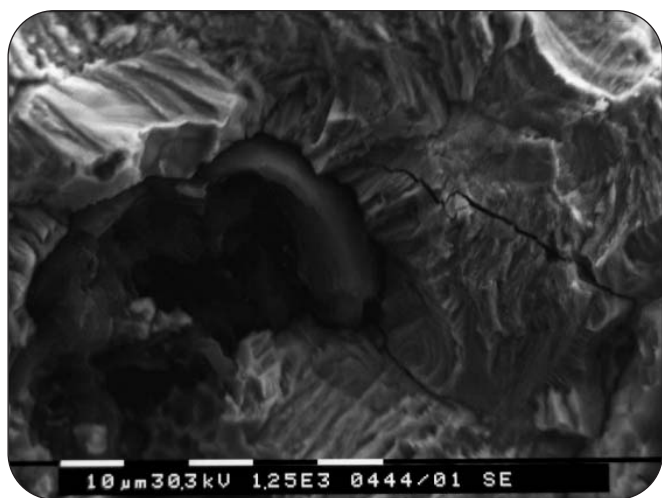


Fig. 10

ADIA ductile iron fracture surface ($R = 0,5; \Delta K = 6$ MPa√m).

Ghisa austemperata ADIA, superficie di frattura ($R = 0,5; \Delta K = 6$ MPa√m).

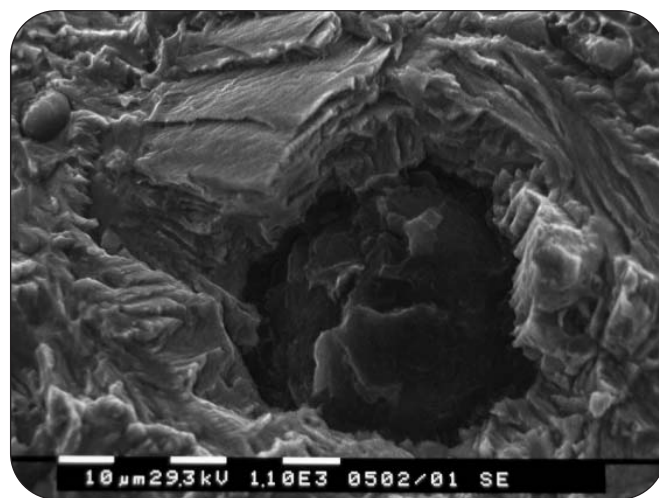


Fig. 11

ADIB ductile iron fracture surface ($R = 0,5; \phi K = 6$ MPa√m).

Ghisa austemperata ADIB, superficie di frattura ($R = 0,5; \phi K = 6$ MPa√m).

approximation error and a measure of the segmentation efficiency: a good segmentation is constituted by a minimum number of disjoint sub-domains with minimal area and regular boundary. Each sub-domain can be defined by means of the level set functions. Consider for simplicity an image with only one object different from the background, therefore there are only two sub-regions: D_1 corresponding to the object, and $D_2 = D/D_1$ corresponding to the background. Let $\emptyset = \{\emptyset_{2,j}\}: D \rightarrow \mathbb{R}$ be a continuous function; D_1 and D_2 can be defined as follows

$$D_1 = \{(i, j) : \phi_{i,j} \geq 0\}, \quad D_2 = \{(i, j) : \phi_{i,j} < 0\} \quad (2)$$

The segmentation boundary is known once the boundary points of D_1 and D_2 are identified. These boundaries have to be defined according to the number of sign changes of \emptyset in a suitable neighbourhood of each pixel. To this aim, in [9] a function $y(\emptyset_{2,j})$ has been defined; it takes value 1 if pixel (i, j) is a boundary point and 0 otherwise. Then the following cost functional can be defined

$$E(c_1, c_2; \phi) = \lambda \sum_{i,j} H(\phi_{i,j})(l_{i,j} - c_1)^2 + \lambda \sum_{i,j} (1 - H(\phi_{i,j}))(l_{i,j} - c_2)^2 + \frac{\alpha}{2} \sum_{i,j} \phi_{i,j}^2 + \mu \sum_{i,j} H(\phi_{i,j}) + \nu \sum_{i,j} y(\phi_{i,j}) \quad (3)$$

where $H(\cdot)$ is the Heaviside function and $\lambda, \alpha, \mu, \nu$ are parameters to be chosen in order to weigh differently the influence of the various terms in the cost functional. In [9] the following necessary and sufficient optimality conditions for (3) have been found

$$c_1 = \frac{\sum_{i,j} H(\phi_{i,j}) l_{i,j}}{\sum_{i,j} H(\phi_{i,j})}, \quad c_2 = \frac{\sum_{i,j} (1 - H(\phi_{i,j})) l_{i,j}}{\sum_{i,j} (1 - H(\phi_{i,j}))} \quad (4)$$

$$\phi_{i,j} = -\frac{1}{\alpha} \left(\lambda p_{i,j} + \mu + \nu \sum_{i,j} [(H(\phi_{i+1,j}) - H(\phi_{i,j})) - (H(\phi_{i,j+1}) - H(\phi_{i,j}))] q_{i,j} \right) \delta(\phi_{i,j}) \quad (5)$$

where $p_{i,j}$ and $q_{i,j}$ are auxiliary functions suitably defined. Relations (4) provides in closed form the optimal values for constants c_1, c_2 , whereas equation (5) can be solved by a recursive scheme [9,13].

ABSTRACT

IMPIEGO DELLA SEGMENTAZIONE MEDIANTE CONTORNI ATTIVI NELL'IDENTIFICAZIONE DEGLI ELEMENTI METALLOGRAFICI E MORFOLOGICI DI INTERESSE NELLE GHISE SFEROIDALI

Parole chiave: ghise sferoidali, analisi di immagine, segmentazione, contorni attivi

Le ghise sferoidali costituiscono una famiglia di ghise piuttosto versatile caratterizzata da un ampio intervallo di proprietà meccaniche che possono essere ottenute mediante il controllo della microstruttura e degli sferoidi. Il controllo della microstruttura della matrice è ottenuto mediante sia il controllo della composizione chimica che del processo di produzione. Si possono avere ghise sferoidali ferritiche, ferrito-perlitiche, perlitiche, martensitiche, bainitiche, austenitiche ed "austemperate". In funzione della microstruttura si può ottenere un'ampia varietà delle combinazioni delle possibili proprietà meccaniche. Per quanto riguarda il comportamento alla frattura, la caratteristica fondamentale di queste ghise è la presenza della grafite sotto forma di noduli che, grazie alla loro morfologia, possono agire come "crack arresters". Ciò consente di ottenere valori di duttilità e di tenacità superiori di assoluto interesse per impieghi per i quali sono previste sollecitazioni elevate, anche variabili nel tempo.

L'analisi della microstruttura dei materiali sino a qualche anno fa veniva principalmente affidata a metodi semi-quantitativi basati su ispezione visiva da parte di esperti di provini metallografici. Solo negli ultimi anni è cresciuto l'interesse in valutazioni che facessero ricorso a tecniche numeriche di analisi di immagine. In questo lavoro il problema dell'identificazione delle caratteristiche morfologiche di elementi quali noduli di grafite, zone dell'attacco chimico e matrice metallica, è stato affrontato con un approccio variazionale denominato segmentazione mediante contorni attivi.

Nel caso delle ghise sferoidali, le immagini ricavabili dall'analisi metallografica al microscopio ottico mostrano, oltre agli sferoidi, alle zone di attacco

chimico e alla microstruttura, profili irregolari e artefatti dovuti alla procedura di acquisizione, che devono essere distinti dagli elementi di interesse. Si propone quindi una procedura automatica di identificazione in grado di riconoscere i profili relativi agli sferoidi distinguendoli dalla matrice metallica e di quantificare quindi sia i parametri morfologici di interesse degli elementi di grafite, sia la distribuzione della matrice metallica (percentuale di ferrite e di perlite).

In questo lavoro è stato affrontato il problema dell'identificazione e della caratterizzazione delle particelle di grafite nelle ghise sferoidali ed il problema della caratterizzazione della matrice, utilizzando una procedura di segmentazione innovativa detta segmentazione mediante contorni attivi. È stata proposta una procedura di identificazione basata su un metodo variazionale in grado di riconoscere i profili relativi ai noduli di grafite, ed identificare i differenti costituenti strutturali nella matrice metallica. La procedura proposta è stata applicata a ghise sferoidali ferrito-perlitiche (per l'identificazione e la quantificazione della matrice metallica) ed a ghise sferoidali austemperate (per la valutazione dello stato di degenerazione degli elementi di grafite. In quest'ultimo caso è stata analizzata l'influenza di tale degenerazione sulla resistenza alla propagazione della cricca di fatica e sui micro-mecanismi di avanzamento. I risultati ottenuti hanno consentito di trarre le seguenti conclusioni:

- la procedura di analisi di immagine proposta consente una caratterizzazione quantitativa ed oggettiva sia delle frazioni volumetriche delle fasi e dei costituenti presenti, sia del livello di degenerazione degli elementi di grafite, evitando la necessità di un particolare addestramento dell'operatore;
- la matrice metallica ha una particolare influenza sulla resistenza alla propagazione della cricca di fatica per elevati valori di R e/o di ΔK , mentre il grado di degenerazione degli elementi di grafite influenza il comportamento a fatica solo per bassi valori di ΔK , qualunque sia il valore di R considerato;
- la presenza di elementi di grafite degenerati implica l'innescio di cricche secondarie che propagano nella matrice metallica.